Sodium Channel Subconductance Levels Measured with a New Variance-Mean Analysis

JOSEPH B. PATLAK

From the Department of Physiology and Biophysics, University of Vermont, Burlington, Vermont 05405

ABSTRACT The currents through single Na^+ channels were recorded from dissociated cells of the flexor digitorum brevis muscle of the mouse. At 15°C the prolonged bursts of Na^+ channel openings produced by application of the drug DPI 201-106 had brief sojourns to subconductance levels. The subconductance events were relatively rare and brief, but could be identified using a new technique that sorts amplitude estimates based on their variance. The resulting "levels histogram" had a resolution of the conductance levels during channel activity that was superior to that of standard amplitude histograms. Cooling the preparation to 0°C prolonged the subconductance events, and permitted further quantitative analysis of their amplitudes, as well as clear observations of single-channel subconductance events from untreated Na^+ channels. In all cases the results were similar: a subconductance level, with an amplitude of roughly 35% of the fully open conductance and similar reversal potential, was present in both drug-treated and normal Na^+ channels. Drug-treated channels spent ~3–6% of their total open time in the subconductance state over a range of potentials that caused the open probability to vary between 0.1 and 0.9. The summed levels histograms from many channels had a distinctive form, with broader, asymmetrical open and substate distributions compared with those of the closed state. Individual subconductance events to levels other than the most common 35% were also observed. I conclude that subconductance events are a normal subset of the open state of Na^+ channels, whether or not they are drug treated. The subconductance events may represent a conformational alteration of the channel that occurs when it conducts ions.

INTRODUCTION

The initial single-channel recordings of Neher and Sakmann (1976) demonstrated that the nicotinic acetylcholine (ACh)–activated channel switches quickly between a closed and a constant conductance level. This observation of quantal conductance levels and rapid switching has since been seen in many other types of channels, and has come to be accepted as the "standard" behavior of ion channels. Exceptions to this standard have also been demonstrated, however. Alamethicin, which was among the first single-channel currents observed (in bilayers), switches between numerous

conductance levels, which are thought to correspond to structural changes of the channel (Gordon and Haydon, 1972; Latorre and Alvarez, 1981). Some native channels also commonly display two or more conductance levels. Potassium channels from sarcoplasmic reticulum show two (Labarca and Miller, 1981), and chloride channels in epithelial cells show up to seven different conductance levels (Krouse et al., 1986). Gamma-aminobutyric acid- (Hamill et al., 1983) and glutamate- (Cull-Candy and Usowicz, 1987; Jahr and Stevens, 1987) activated channels display three or more conductances, and glutamate channels alter the conductance level that they reach depending on the transmitter substance that is bound.

Even channels that typify the open/closed pattern display occasional subconductance levels (sublevels). ACh-activated channels show rare openings or closings to one or more sublevels (Hamill and Sakmann, 1981; Auerbach and Sachs, 1983; Colquhoun and Sakmann, 1985). Nagy (1987) reported sublevels for drug-modified Na^+ channels, and Prodhom et al. (1987) have shown sublevels for Ca^{++} channels. The quantitative analysis of such sublevels can provide important information about the channel's pore. For example, Prodhom et al. (1987) showed that the binding of H^+ ions within the Ca^{++} channel pore causes a reduction of the current to a sublevel, and their quantitative analysis of the sublevel occurrence was used to determine the binding constants of H^+ for the channel site.

The need for better quantitative analysis of Na^+ channel sublevels became apparent during experiments to quantify the kinetics of Na^+ channels that had had their inactivation removed by treatment with the drug DPI 201-106. Under some of my recording conditions, sublevels were particularly prominent. Without a thorough knowledge of the frequency and amplitude of subconductance states, I could not measure kinetic parameters of the channels accurately. However, the techniques that were available for such analyses were less than optimal for various reasons. One common method, amplitude histogram analysis, simply orders the histogram entries by the amplitude of the current at each time point. Although easy, this method's resolution is no better than the background noise, and it does not distinguish between points taken during sublevels and those points in transition between the main levels. A much more sophisticated analysis proposed by Colquhoun and Sigworth (1983) fits each amplitude with a presumed event convoluted with the measured response of the system. The technique yields excellent fits, but it is difficult to implement, tedious to perform on large quantities of data, requires excellent signal to noise, and yields amplitude estimates whose accuracy varies from one event to the next. Nagy and Bagany (1986) suggested an automatic "filtering" of single-channel data by setting a variance threshold that establishes individual transitions, but he had no rigorous criteria for accepting or rejecting individual sublevels.

In this paper I use a new method, based on the variance-current structure of single-channel data, to describe subconductance levels in drug-modified and normal Na^+ channels. At least one sublevel occurred in drug-modified Na^+ channels. It was reached from both the open and closed states, had a reversal potential similar to that of the fully open state, and occurred as a relatively constant fraction of the amount of time the channel spent in the open state. Unmodified Na^+ channels at low temperature also had sublevels similar to those of the drug-modified channels.

METHODS

Preparation

All recordings were made on skeletal muscle fibers dissociated from the flexor digitorum brevis muscle of the mouse (BALB/cByJIco strain; IFFA CREDO, L'Arbresle, France). The muscles were dissected from the sole of the hind paw, pinned in a small dish, and bathed in physiological saline (PS) solution (in millimolars: 140 NaCl, 5 KCl, 0.2 CaCl$_2$, 0.2 MgCl$_2$, 10 HEPES, 10 dextrose, titrated to pH 7.4 with NaOH). The muscles were subsequently bathed for 90–120 min at room temperature in 6 mg/ml collagenase (Sigma type 1A; Sigma Chemical Co., St. Louis, MO), then for 30 min in 1 mg/ml protease (Sigma type VII), both of which were dissolved in PS. After a brief rinse with PS, the muscles were transferred to the "relaxing" solution, which consisted of (in millimolars): 130 CsAspartate, 5 KCl, 3 MgCl$_2$, 5 Na$_2$ATP, 10 HEPES, 30 dextrose, 0.1 EGTA, 4% dextran T70, titrated to pH 7.4 with CsOH. After a roughly 15-min equilibration, the cells were dissociated by gentle trituration in a fire-polished Pasteur pipette.

Small aliquots of the dissociated muscle fibers were transferred to a chamber consisting of a 35-mm tissue culture petri dish, and were allowed to settle to the bottom. The chamber was mounted on an aluminum block that was cooled by Peltier elements. The bath temperature was measured near the cells with a small thermocouple element. Patch recordings were made by standard techniques. In brief, pipettes were pulled from borosilicate capillary tubes, coated with Sylgard, and fire polished to a final diameter <1 μm (5–10 MΩ resistance). The pipette was filled with filtered PS. Gigaseals could usually be obtained quickly by gentle suction.

Patch currents were amplified with a List EPC-7 patch clamp (List Electronic, Darmstadt, FRG), and were filtered at 2–3 kHz with a Bessel-type low-pass filter. An IBM-PC-AT–compatible computer was used to control the membrane potential of the patches, and to sample the currents at regular intervals. All recordings were made in the cell-attached configuration. Since the resting potential of the cells in the Cs-relaxing solution was quite low (<5 mV), the potentials given here can be considered to be close to the transmembrane potential of the patch.

Enantiomers of DPI 201-106, 4-[3-(4-diphenyl-methyl-piperazinyl)-2-hydroxypropoxy]-1H-indole-2-carbonitrile, were a gift of Dr. Scholtysik, Sandoz Inc., Basel, Switzerland. Stock solutions of the drug were made in ethanol, since it dissolved poorly in PS. However, to avoid potential direct effects of the ethanol solvent on the membranes under study, ~2 μg of DPI's s-enantiomer were dried into the chamber before the application of 1–2 ml of the Cs-relaxing solution, yielding a final concentration of much less than 2 μM (only a small fraction of the applied drug redissolved in the experimental medium). The chamber, bath electrode, and thermocouple covering were renewed for each experiment to assure that no drug was accidentally present in drug-free experiments.

Analysis Method

The initial goal of a quantitative analysis of channel conductance is to identify the magnitude and relative frequency of the current levels that an individual channel can reach. If a channel's current could be recorded without background noise, then periods without channel activity will have both current and variance equal to zero. When a channel is active, there would be times during which a constant current flows at a particular current level. Thus, current levels may be defined as periods of time in which the variance of the current is as low as when no current is flowing. If the records have background noise, then current levels

would be the mean current observed during periods in which the variance is no more than that of the background noise. The variance-mean analysis that I used is based on this definition.

The analysis consists of sliding a "window" of width N sample points over a discretely sampled data record, and calculating the mean, $\langle I \rangle$, and the sample variance, s^2, of the points within the window. For the studies presented here the window was advanced by one point for each pair of variance-mean points. The resulting values were plotted against one another, as shown for a simulated, noise-free, two-state channel in Fig. 1 A. In this case N was 20. During periods in which the channel was closed, the $\langle I \rangle$ and s^2 were both zero. During periods where the channel was open, $\langle I \rangle$ was equal to i, the single-channel current, and s^2 was again equal to zero. At times when the window contained one or more points of transition between the two states, s^2 was greater than zero, and $\langle I \rangle$ had values between the two current levels. The variance-mean plot therefore consisted of a roughly parabolic curve with two node points at the current levels reached by the channel. Events that were shorter than the window width, as well as very brief events that had been attenuated by the filter, yielded incomplete parabola-like curves that often deviated from the main curve at their final points, as can be seen in Fig. 1, A and B. Such brief events had, nevertheless, substantially increased variance compared with those that were fully open or closed.

If sublevels exist in the data, then an intermediate node may be observed, in which the points within the window have an s^2 equal to zero with an intermediate $\langle I \rangle$. Such an example, also for synthesized, noise-free data in which a sublevel was reached from the open state, is shown in Fig. 1 B. The existence of the sublevel is clear. The direction of the transitions into and out of the sublevel can be determined from the trajectory of the variance-mean curves.

Actual data generally consists of such channel signals superimposed on background noise. In such cases the estimate of $\langle I \rangle$ and s^2 are randomly distributed. For Gaussian noise that is uncorrelated, for example, $\langle I \rangle$ also has a Gaussian distribution with a standard deviation:

$$\sigma_{\langle I \rangle} = \frac{\sigma_b}{\sqrt{N}},$$ (1)

where σ_b is the standard deviation of the background noise. The estimates of variance s^2 have a χ^2 distribution with $N - 1$ degrees of freedom (Bendat and Piersol, 1986) such that:

$$\frac{s^2}{\sigma_b^2} = \frac{\chi_n^2}{n},$$ (2)

where $n = N - 1$. The result of background noise is thus a blurring of the variance-mean curve along both axes, as shown in Fig. 1 C. Nevertheless, the primary pattern is still clearly visible.

To analyze such data quantitatively, a criterion is required for distinguishing which points belong to a particular level. For the present analysis I have used

$$s^2 \leq \sigma_b^2$$ (3)

as the condition to accept mean currents, $\langle I \rangle$, as representing a valid current level. This criterion was chosen because (a) it is conservative, excluding half of the points at any level, and also excluding virtually all transition points, and (b) the fraction of points excluded is approximately the same for all values of N since

$$\text{Prob}\left(\frac{\chi_n^2}{n} \geq 1\right) \sim 0.5.$$ (4)

Fig. 1 *D* shows a histogram of all current amplitudes, $\langle I \rangle$, (from the data shown in Fig. 1 *C*) that satisfy the criterion of Eq. 3. The existence of a single sublevel, in addition to the two main levels, is clear. The resolution of such a histogram is much higher than that of the amplitude histogram (shown in the inset for comparison) because the variance of the current estimates at each level is reduced by *N*, and because transition points between levels are excluded.
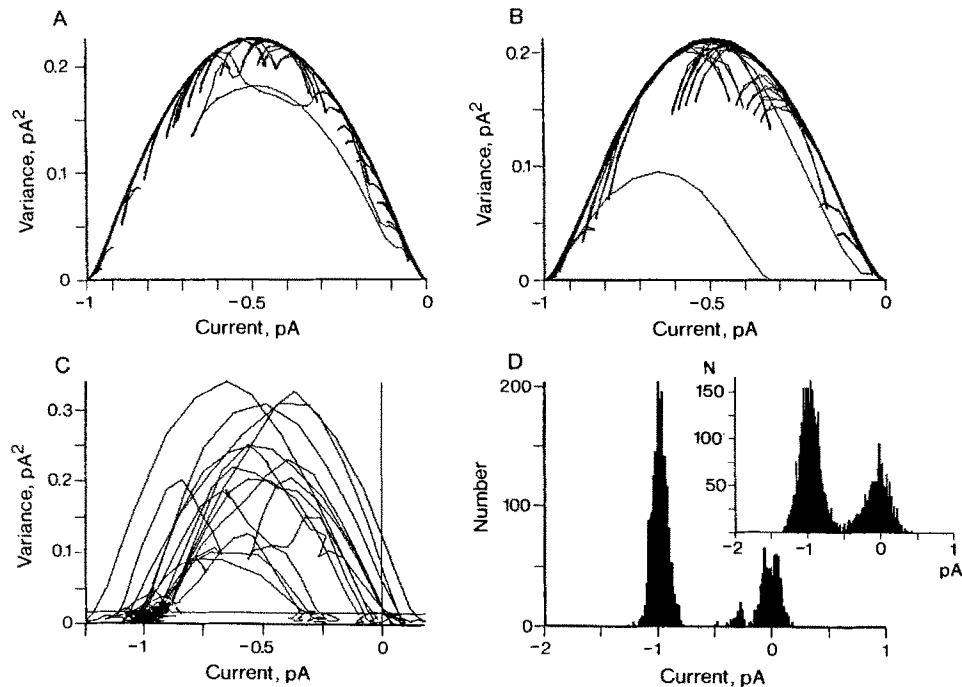

FIGURE 1.   Levels analysis on simulated single-channel data. The activity of one channel with an inward (negative) current of 1 pA when open was simulated using pseudo-random numbers. The lifetime in each of the open, closed, and subconductance states was determined as $-\ln(R)/K$, where *R* is a random number between 0 and 1, and *K* is the sum of the rates leaving the state. The simulated signals were first produced with a sample rate of 500 kHz, then digitally filtered to 3 kHz before resampling at 10 kHz. (*A*) Variance-mean plot from simulated currents with no noise and no subconductance states. The window width was 20 sample points, and its position was advanced one sample point for each variance-mean estimate. Sequential points have been connected by straight lines. (*B*) Variance-mean plot of a simulated channel with a subconductance level of 0.33 pA, but no noise. Window width was 20 points. (*C*) The same model as in *B*, but with added Gaussian noise giving a signal-to-noise ratio of ~7. The window width used here was 10 points. The solid horizontal line above the abscissa is the variance of the background noise, which was used as a threshold for inclusion of amplitude estimates in the levels histogram. (*D*) The levels histogram produced by 400 ms of channel activity using the simulation from *C*. The presence of periods in which the variance was lower than that of the background noise alone at mean currents corresponding to the subconductance level can be clearly seen. In contrast, the stanard amplitude histogram (inset), with one entry for each sample point, has little ability to resolve the sublevel.

Several points are worth noting for the practical application of the method. (a) The levels histogram does not, by itself, contain information that distinguishes between the levels caused by two or more channels from multiple levels of a single channel. Such distinctions must rather be drawn on the basis of the original data. For example, if two identical channels are simultaneously active, then the levels histogram would contain entries at zero, one, and two times the current through the single channel. The occurrence of multiple channels is common in patch recording, and can be verified with standard techniques, such as determining that the frequency of overlapping currents fits Poisson statistics (Neher and Sakmann, 1976). Patches with two different channel types would give rise to entries in the levels histogram that might appear similar to subconductance levels of a single-channel type. The simultaneous activity of independent channel types makes specific predictions, however, that can be tested in the data. For independent channels the magnitude of the current steps due to channel opening or closing would be almost exclusively equal to the amplitude of each channel's current, not to their difference (except in the rare cases of simultaneous transitions of opposite polarity). In addition, the activity of the two independent channel types would not be coupled, so that each channel type should be observed to function when the other is inactive. Since neither of these conditions is fulfilled in my data, I conclude that the minor components are due to true subconductance levels.

(b) Although the presence of currents from simultaneously active channels does not invalidate the levels histogram analysis, the greater the level of activity, the larger the potential for diverse peaks, which are due to the possible combinations of the levels from each of the active channels. Therefore, the interpretation of the analysis is simplified when the channel activity is low.

(c) Currents will usually only satisfy the condition for inclusion as a level if they are long enough to include a segment of length N after the transition is complete. This means that the minimum length of a measured level is N plus the number of sample points required for the system to respond to a current jump. For data sampled at five times the cutoff frequency (f_c) this condition is met at $\sim N + 2$ points. For example, I used $N = 5$ for my records that were filtered at 2 kHz and sampled at 10 kHz. The minimum event duration that would cause an entry into the levels histogram was thus 700 μs. Events with length 800 μs would generate two entries, etc. Therefore, the relative area under the peak is only approximately proportional to the occupancy of a given level. The more rapid the kinetics, the greater the error in this relation. Since the dwell time at each level may be different, significant bias may be present for a given sampling rate and window width. Events that are too short to resolve at a given window width are not entered into the levels histogram, but can be seen as incomplete parabola-like curves in the variance-mean plots. Their presence indicates that significant numbers of openings are being missed, and that the data should also be examined at narrower window widths, if possible.

(d) The "best" value of N cannot be prescribed a priori. It depends on numerous factors, the most important of which are signal-to-noise ratio, spacing of the sublevels, the average dwell time at the levels of interest, and the match between f_c and the sampling frequency. Finally, the desired application of the analysis (quantitative measure of the levels' amplitude vs. relative frequency of events at a particular level) may influence the choice of N. In general, it is best to systematically vary N for a given set of data. In doing so, one can obtain an empirical estimate for its useful range of values. In addition, by measuring the rate at which the number of entries in a particular level decrease as a function of N, a rough estimate of the average dwell time at each level can be obtained. For the present study I have generally used values of N between 5 and 20.

(e) In general, single-channel data are "oversampled," i.e., sampled at greater than the Nyquist frequency two times the f_c of the filter. In this condition, the current of neighboring

data points are correlated with one another and thus:

$$\sigma_{(i)} > \frac{\sigma_b}{\sqrt{N}} .$$ (5)

For data sampled at five times the f_c, the effective value of N is roughly 50% of the true value. As the degree of oversampling increases, the effective N decreases, ultimately leading to a breakdown of the relationships cited above when N is small and the oversampling is large. Therefore, oversampling should be restricted when using this analysis.

(f) If the current through the open channel is noisy due to rapid block of the open channel or to other factors, then the variance during this open state will never be as low as that for the baseline. Although this appears not to have been a major factor in the present work, perhaps because of a limited signal-to-noise ratio, such open-channel noise has been observed in a number of channel types. Although such open-channel noise would preclude the selection of levels based on the criterion of the background noise variance, as described here, the variance-mean plots would be useful to quantify the open-channel noise, and to distinguish between rapid "flickery" noise and that produced by switching between two or more closely spaced sublevels. Furthermore, the threshold for histogram inclusion might be appropriately modified to permit levels histograms to be constructed based on alternative definitions of a current level.

(g) A steady, flat, baseline is important for maximum resolution of levels. In many cases I was able to subtract the average of blank traces to obtain such a baseline. In some data the baseline shifted slowly between records. To obtain the maximum resolution I fitted the baseline component of the levels histogram with a Gaussian curve, and shifted the histogram so that the maximum of this curve was at zero current. Shifted histograms could then be averaged with each other without the danger of blurring the individual components.

RESULTS

DPI 201-106–treated Channels Have Sublevels

The drug DPI 201-106 has been shown to enhance late Na^+ channel currents in cardiac and other tissues (Scholtysik et al., 1985; Kohlhardt et al., 1986; Romey et al., 1987). It appears to work by inhibiting the channel's fast inactivation, possibly by increasing the channel's spontaneous rate of switching to their noninactivating mode of activity (Patlak and Ortiz, 1986). The s-enantiomer is particularly active in this regard (Romey et al., 1987). I became interested in using the drug as a tool to study the kinetics of single, noninactivating Na^+ channels, and thus tried it on Na^+ channels in the mouse skeletal muscle.

The effect of DPI in this tissue was similar to that reported in cardiac muscle. The rapidly inactivating portion of the Na^+ conductance was somewhat inhibited, and the channels had a much higher probability of producing prolonged burst-like behavior. Two examples of the currents of treated channels in a patch at 15°C are shown in Fig. 2. They were selected from current responses to 200-ms pulses that were applied at 5-s intervals. The holding potential was -120 mV, and the pulse potential was -50 mV. In contrast to the responses without the drug, the proportion of traces with late activity was high, which permitted the efficient collection of such events.

The "closure" of the channel to conductance levels other than zero current can

occasionally be seen in such data. Several examples, selected from the traces, are shown at higher resolution in Fig. 2. However, at 15°C the closures to sublevels observed were rare and usually quite short, and thus not easily identified by casual examination. I therefore used the variance-mean technique described above to study further the occurrence of sublevels in the data.

Fig. 3 A shows a plot of the variance vs. mean behavior for a section of the first of the DPI-induced bursts shown in Fig. 2. Most transitions were between the main current level of 2.0 pA and the closed state. The average variance of the open state was as low as that of the closed state, indicating that little partially resolved open-channel noise contributed to the current. Occasional excursions to a sublevel that had an amplitude of roughly 0.6 pA can also be seen to occur from both the open and the closed state. The variance during some of these sublevel events also
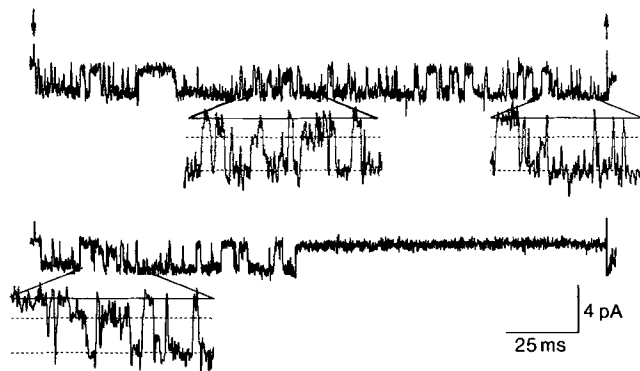
4 pA

25 ms

FIGURE 2. Bursting currents from DPI 201-106–treated channels have sublevels. Two bursts of openings at 15°C from a patch of mouse muscle membrane treated with the s-enantiomer of DPI 201-106 are shown. The data were filtered at 3 kHz and sampled at 20 kHz. The arrows indicate the application and removal of the test pulse to −50 mV from a holding potential of −120 mV. The insets show sections of these traces at higher resolution (the calibration for the insets is 2 pA and 8 ms). The solid line in the insets represents the average zero-current level, and the dashed lines show the position of the main open and the subconductance amplitudes measured on the summed levels histogram of this patch (Fig. 3).

approached that of the baseline, indicating that they are not likely to have occurred as a result of rapid flickering between the open and closed conformations. A number of events can also be seen in which the variance rises to a maximum and starts to fall again, but does not reach the threshold variance. These curves are the result of events that were too brief to resolve fully. They indicate that the analysis was limited by the rapidity of the kinetics that were being studied.

Despite the temporal limitation under these conditions, the summed levels histograms from several such bursts had a characteristic form, as shown in Fig. 3 B (shown here in semi-log scaling to simultaneously display main and the much rarer sublevel peaks). The closed level was symmetrical, with a roughly Gaussian distribution. The fully open level had an asymmetrical form, with a tail on its lower current side. Its width was also greater than that of the closed level. Sublevel entries were

largely absent from a region of ~50–80% of the fully open level, then rose to a peak at about 35% of the open level. There also appeared to be more entries between this sublevel and the closed level than was expected for the sum of two Gaussian components with the same standard deviation. Such asymmetries of the levels histogram might have been due to variation between channels, or to additional unresolved levels.

To observe the sublevel transitions more clearly, I studied the currents through the DPI-treated channel at temperatures between 0 and +2°C. Fig. 4 *A* shows an
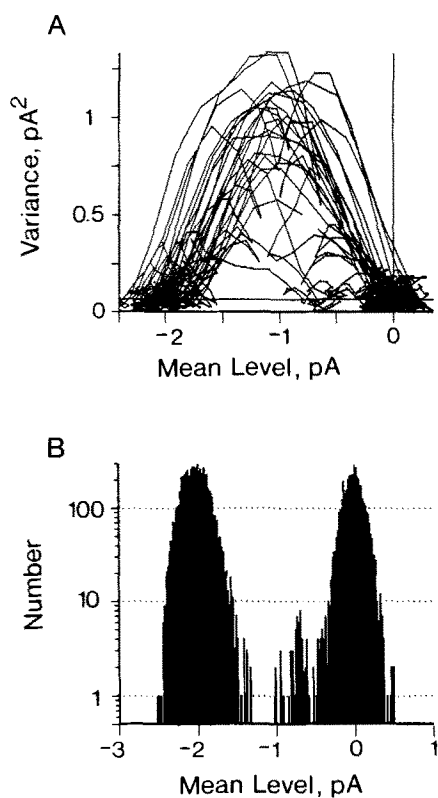
FIGURE 3.   Levels analysis of bursts at 15°C. (*A*) The variance-mean plot of a portion of the top burst shown in Fig. 2. The horizontal line above the abscissa is the variance of the background noise alone. The variance during the open state is as low as that of the baseline, indicating no resolvable open-channel noise. Several events can be seen in which the variance falls below this threshold during subconductance events. Transitions between both the open and sublevel, as well as the closed and sublevel, can be seen. The window width used here was 10 points, corresponding to 500 μs. It was advanced one sample point for each estimate. (*B*) The summed levels histograms of eight bursts from the same patch, including those shown in Fig. 2. The log of the number of entries has been plotted on the ordinate to display both the peaks and the small sublevel component. The baseline peak is well fitted by a single Gaussian curve, while that of the open state is markedly asymmetric. Note also the asymmetry of the sublevel entries. The arrows indicate the position of the dotted lines shown in Fig. 2.

example of the currents produced by a DPI-treated channel at 0°C. Fig. 4 *B* shows the summed levels histogram from 14 such bursts in the same patch. The existence of a small component due to the occurrence of sublevels is now clearly evident in the histogram. In this case, the number of entries in the sublevel portion of the histogram was 3.2% of the number in the primary open state.

The overall form of the levels histogram was the same as that found at higher

temperatures. The open level had a broader distribution than the closed level. In many experiments it also had an asymmetric shape. In addition, the sublevel peak was also centered at ~35% and was broader than the closed level. The lowering of the temperature therefore did not seem to have altered the pattern of sublevels greatly.

The subconductance levels appeared to be associated directly with Na^+ channel activity, and were not due to the artifactual overlap of a second, smaller channel current. Several different types of observation support this finding. First, in traces where no Na^+ channel was active, the levels histogram showed only the baseline histogram, as shown in Fig. 4 C. Second, as discussed in the methods, the temporal
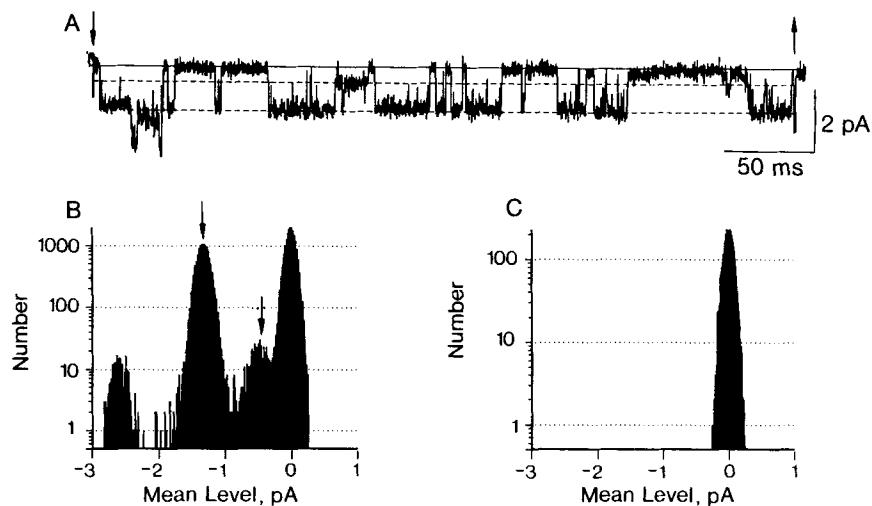

FIGURE 4.   Subconductance levels in DPI-treated channels at 0°C. (A) An example of a burst of Na^+ channel openings at a low temperature, showing a long sojourn into the subconductance level. As above, the arrows show the application of the test pulse to −50 mV, and the dotted lines indicate the peaks of the open and sublevel components in the summed levels histogram. (B) The levels histogram summed from 14 individual bursts in the same patch. Additional levels can be seen to the left due to the simultaneous activity of two different channels. The arrows indicate the amplitudes used in A. (C) The levels histogram from 400 ms of a representative trace of the same patch in which no channel was bursting. No events, other than those of the background component, can be seen.

sequence of the data did not fit the pattern of two independent channel types. Subconductance events, for example, were often observed to be entered from the main state, but to exit to the closed state (and vice versa). Finally, the amplitude and the frequency of occurrence of the sublevel were directly related to the properties of the main current level, as seen below.

The peak of the sublevel component in the levels histogram was a constant fraction of the main level current over a broad range of potentials. Fig. 5 shows the current-voltage characteristics of the main and sublevel components in the levels histogram. The slope conductance for the main level was 16.0 pS, while that of the

sublevel peak was 6.1 pS. These values compare with 23.5 and 9.2 pS obtained at 15°C. In all cases the extrapolated zero-current intercept of the single-channel currents lay between +30 and +45 mV. (In unpublished experiments, the channels were shown to rectify in the nonsymmetrical conditions used here, such that the current-voltage relation would have been better fitted by a Goldman-Hodgkin-Katz relation. The extrapolated zero-current potential is used only as a rough indication of the current-voltage properties.)

The gating of DPI-treated channels was voltage dependent, with longer open times and shorter closed times produced by increasing depolarization (data not shown). This is directly analogous to the gating during spontaneous bursts (Patlak and Oritz, 1986), or to that produced when Na^+ channel inactivation is chemically removed (Vandenberg and Horn, 1984). Thus the relative proportion of the time spent at the open level increased with depolarization compared with the closed level, as seen in Fig. 6, *A–D*. The number of entries at the sublevel also increased with increasing depolarization, but the ratio of sublevel to open level entries
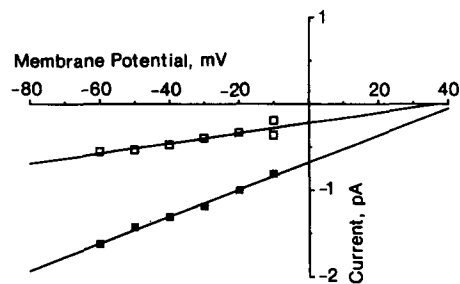

FIGURE 5. Current-voltage relation of the main and the subconductance state. Test pulses were applied to voltages between −60 and −10 mV to patches containing DPI-treated channels at 0°C. The current values at the peak of the main conductance (filled squares) and of the subconductance (open squares) components in the levels histogram are shown. The values used correspond as well to those shown on the histograms with arrows, and to the dotted lines in the data traces.

remained constant (within the limits of accuracy of these measurements) at ~3% over the range of potentials that I studied, as shown in Fig. 6 *E*. The sublevel appeared, therefore, to be more closely related to the open, rather than to the closed conformation of the channel.

Since the variance-mean method as implemented here is insensitive to events shorter than the window width, brief openings and sublevel events do not contribute to the levels histogram. It is of interest, however, to determine what the ratio of sublevel to open level would have been if no events had been missed. To determine this value, I measured the ratio at various window widths on the same data. For example, for the data shown in Fig. 6 *B*, the sublevel to open ratio was 3.1% using a window width of 500 μs, 1.8% for a window of 1 ms, and 1.0% for a window of 1.5 ms. These values are well described by a single exponential function of the window width. When this exponential was extrapolated back to zero, it gave an estimate for the original extent of sublevels in the data. In this case, that value was ~6%.

Untreated Channels Have Similar Sublevels

Subconductance levels have been previously reported for Na^+ channels treated with a number of substances that remove inactivation (Green et al., 1987; Nagy, 1987; Urban et al., 1987). An important unanswered question is whether such sojourns to
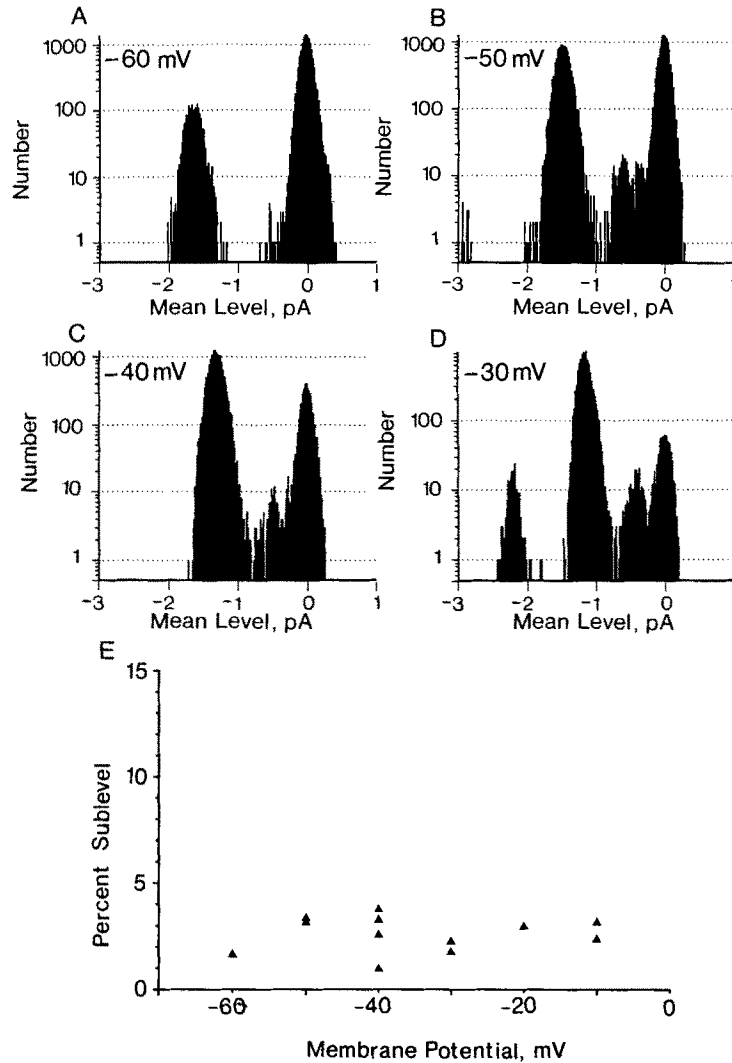

FIGURE 6. Occupancy of the subconductance level as a function of membrane potential. (*A–D*) Summed levels histograms for DPI-treated channels from one patch at 0°C. The test potentials, between −60 and −30 mV, are indicated on each of the panels. At −60 mV the channel was mostly closed, and sublevels were rare. At −30 mV the channel was mostly open and had a prominent subconductance peak. (*E*) The ratio of the area under the subconductance peak to that under the main peak for the estimate of several patches under similar conditions. This ratio showed no significant change over the range of potentials that were measurable.

subconductance levels are a normal property of Na^+ channels, or if they are induced in some way by the drug treatment. To study this question, I recorded the currents through untreated Na^+ channels at low temperature. At 0°C the single-channel events of Na^+ channels were slow enough that most events could be clearly
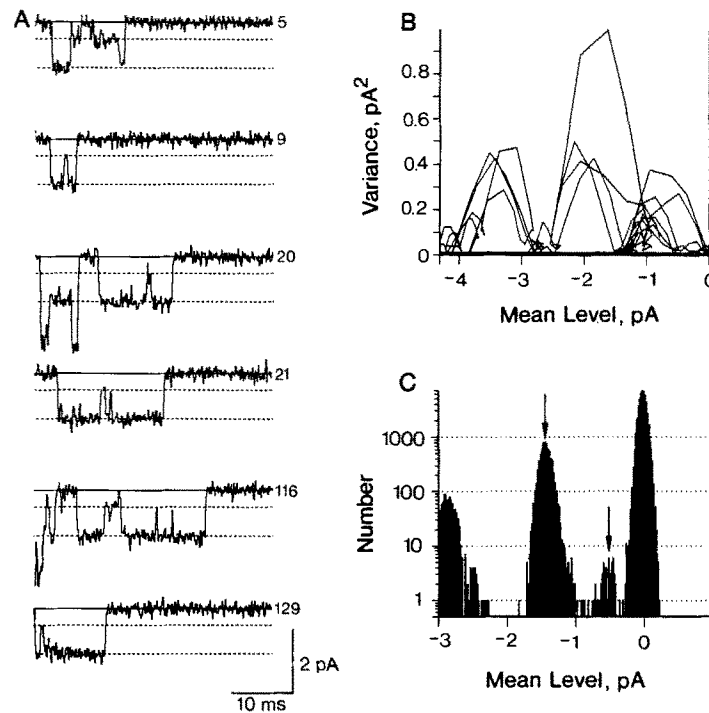

FIGURE 7. Subconductance events in untreated channels at 0°C. Na^+ channels were recorded in a chamber that had never been exposed to drug (including new ground electrode and temperature probe). Bursts like those seen in DPI were not observed, and the channels inactivated quickly during the 40-ms test pulses that were applied. (A) Selected currents from an ensemble of 308 pulses in one patch that were applied at 1 Hz from a holding potential of −100 to a test potential of −50 mV. The numbers to the right of each trace indicate the pulse number. The pulse was applied at the start of the traces and ended just after the end of the currents shown. Blank traces were averaged and subtracted from the traces shown for maximal baseline correction. The solid line indicates zero current, and the dotted lines are the peaks of the components on the levels histogram shown in C. (B) The variance-mean trace from one pulse in which several channels were active. The occupancy of each unitary level is apparent, as is a brief sojourn to a subconductance level. The variance of the background noise is indicated by the solid line just above the abscissa. (C) The summed levels histogram from 308 pulses. The arrows indicate the values used to draw the dashed lines in A.

resolved before the channel inactivated. This permitted me to examine the openings for sublevels, and to use the variance-mean analysis.

Fig. 7 A shows selected examples of the currents through single Na^+ channels at 2°C. The sublevels that were reached during these records are easy to identify and

unambiguous. These records thus demonstrate that the existence of sublevels was not a unique property of drug-treated channels. The quantitative analysis of these traces permitted a more detailed comparison of sublevels in drug-treated and normal Na^+ channels at low temperature.

Fig. 7 B shows one example of a variance-mean analysis of the Na^+ channel currents produced by a pulse to −40 mV. The occurrence of up to three simultaneously open channels can be seen, as well as the occasional brief occupancy of a sublevel between the zero current and the first level. The summed levels histogram from 308 sequential pulses in this patch shows the sublevels clearly as well, as shown in Fig. 7 C.

The levels histogram had a "signature" similar to that seen in DPI-treated channels. The main level had an asymmetric distribution, and a peak sublevel occupancy was found at about one third the main level's current. Finally, the sublevel distribution was often asymmetric as well, with an increased number of events between its
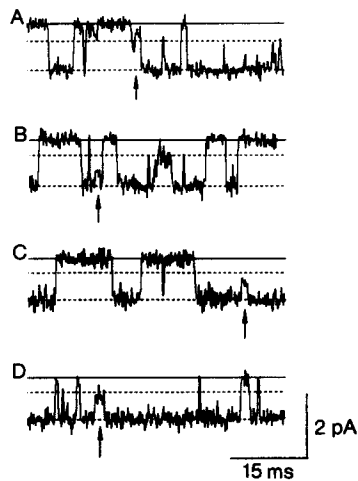

FIGURE 8. Sublevel amplitudes different from the most common at 35%. Sections of DPI-induced bursts at 0°C from two different patches illustrate the diversity of possible subconductance events. (A and B) Bursts from one patch at −50 mV showing sublevel occurrences (arrows) at 20 and 70%. (C and D) Bursts from a different patch at −40 mV showing two other instances of unusual amplitudes. In these cases the amplitudes reached were ~50 and 40% of the main conductance level. The occupancy of particular levels did not appear to be a function of membrane potential.

peak and closed levels. In addition, the current-voltage characteristics of the sublevel peak were virtually identical to those of DPI-treated channels at the same temperature. The fraction of sublevel entries was somewhat lower than that for the drug-treated channels, however (~1% of main level entries in control conditions).

Three or More Sublevels Can Be Detected

The simplest hypothesis that I examined to explain my observations was that there was a single sublevel with an amplitude 35% of the main level. This hypothesis failed to explain several of my results. First, the shape of the levels histogram was not the simple sum of three Gaussian components (base, sublevel, and main) that this hypothesis would predict. Second (and more important), current levels were observed that could not have been caused by the three most common levels, nor by a rapid switching between them. Fig. 8 shows four such examples, taken during records of the currents of DPI-treated channels at 0°C. The dashed lines in the figures show the amplitude of the 100 and the 35% conductance levels. Fig. 8, A and B

show traces at −50 mV. The arrows indicate subconductance events at 20 and 70%. Fig. 8, *C* and *D* show currents (at −40 mV) to 50 and 40% of the main current. Although such events were rare, they appeared in each patch studied. The occurrence of sublevels other than at 35% could explain the characteristic form of the averaged levels histogram. Therefore, the minimum hypothesis that can explain my observations is one in which the Na^+ channel can have a range of possible subconductances, with the most common of these occurring at ~35% of the main conductance level.

DISCUSSION

This paper presents a quantitative description of the subconductance levels that a Na^+ channel can reach during its function, both in its normal state and when treated with the drug DPI 201-106. In addition to illustrating the sublevel currents directly, it uses a new method to quantitate the amplitude and frequency of the sublevel events. The work shows that one or more sublevels is occasionally occupied by the Na^+ channel, in addition to its normal fully open and closed levels.

The technique that I present here is based on the concept that a channel's pore can provide a constant-conductance pathway for a finite period of time. If so, the variance of the current during this time should be no more than that of the baseline, when no current is flowing. By sorting records of channel activity of those instances when this condition is fulfilled, one can automatically, yet rigorously, identify possible current levels for a channel's conductance pathway. The technique is advantageous because it excludes points during current transitions and events that are too short to permit accurate measurement of the current level. In addition, it improves the resolution of individual levels by averaging a constant number of points. It is easy to implement, and relatively quick. It may also be useful for helping to identify transitions between current levels in data that have multiple sublevels, and for quantitating the time spent at each level. Its primary disadvantages are that it is insensitive to events shorter than the window width, and that alterations in the baseline can degrade its resolution.

Subconductance levels have been previously reported for the Na^+ channels in the presence of a variety of inactivation-removing agents. Na^+ channels in bilayers that were treated with veratradine opened only to a level much smaller than that of BTX-treated channels (Garber and Miller, 1987). In addition, Urban et al. (1987) have reported that aconitine produces openings to an amplitude less than half of that produced by veratradine (also in bilayers), and that batrachotoxin (BTX)-treated channels open to the main level as well as occasionally to the levels produced by the other two toxins. Green et al. (1987) also demonstrated subconductance levels of 20–30%, and 30–50% of the fully open current in BTX-treated channels in bilayers. Chinn and Narahashi (1986) saw subconductance events to 66% of the open level in 5% of the deltamethrin-treated Na^+ channels in neuroblastoma. Similarly, Nagy (1987) has reported several different sublevels in Na^+ channels of neuroblastoma cells treated with chloramine-T, sea anemone toxin, and scorpion toxin. He saw currents at 28, 55, and 130% of the main level. Subconductance events longer than 0.56 ms constituted <4% of the open time of these channels.

Few reports of sublevels in untreated Na^+ channels exist, probably because the

openings are very short due to the fast inactivation process. Cachelin et al. (1983) reported openings of Na^+ channels in tissue cultured cardiac muscle to an amplitude ~60% of the normal current. Scanley and Fozzard (1987) have reported similar openings in dissociated Purkinje cells. These authors concluded that the low conductance openings represented a separate type of channel. Indeed, considerable evidence points to multiple types of Na^+ channels in various tissues (e.g., Noda et al., 1986; Weiss and Horn, 1986). In contrast, Nagy et al. (1983) reported that amplitude histograms of the fast openings required Gaussian components with mean amplitudes of 50, 80, and 100% to explain the observed currents. They therefore speculated that the normal openings also exhibited sublevels.

My observations confirm, at least qualitatively, these previous reports of subconductance levels for drug-treated Na^+ channels. In addition, by measuring Na^+ currents at very low temperatures I was able to show sublevels that could not have resulted from multiple populations of channels. The sublevel's "signature" (i.e., the pattern of entries in the summed levels histogram) was very similar in the three conditions that I studied: DPI treated at 15°C, DPI treated at 0°C, and untreated at 0°C. It appears, therefore, that neither temperature, nor removal of inactivation with DPI alters the quantitative pattern of sublevels for the Na^+ channel. I have also reexamined older data of spontaneous bursts of Na^+ channels from frog skeletal muscle (Patlak and Ortiz, 1986) for the presence of sublevels. These events also fit into the pattern of sublevels that I report here. The sublevel component was asymmetrical and had a peak at amplitudes about one third of the fully open level. Sublevels also occurred at a rate similar to that in DPI-treated channels of mouse muscle (unpublished observations). The analysis that I have used thus produces a consistent picture of the possible sublevels for skeletal muscle Na^+ channels.

The quantitative differences between the values reported here and in the literature for Na^+ channel sublevels may be due to several factors: Na^+ channels from different preparations may, of course, express different properites. In addition, the treatment of a channel with particular drugs may affect the probability of occurrence of a particular substate. For example, veratradine leads to a reduced conductance that persists for long periods, spanning many openings and closings of the channel's gates. Such changes must be due to relatively stable alterations of a channel's pore structure. These long-term sublevels might occur by a mechanism that is different from, though perhaps related to, that which produces the transient events seen in the absence of drug, or with DPI 201-106. Finally, sublevel amplitudes may themselves be quite variable from time to time. For example, Green et al. (1987) reported that the current level of one of their "flickery" sublevels varied from channel to channel, as well as with time in a single channel. The short sublevel events that occur in native Na^+ channels might vary in a similar way. Since these events are rare, the analysis of large amounts of data would be required to determine the probability distribution of a particular level.

The implications of sublevels for the Na^+ channel's role in cellular excitation are probably small. These events are relatively rare, and very brief. On the other hand, such events can provide useful insights into the channel's permeation structure. Hunter and Giebisch (1987), for example, have proposed a multipore structure of K^+ channels in a renal tubule, where the whole channel can be gated, as well as each subchannel, thus producing what appears to be a main conductance and subcon-

ductance levels. Since the conductance levels that I observe are not evenly spaced, however, the multipore model of Hunter and Giebisch appears an unlikely description of Na^+ channels. An alternative mechanism proposed by Prodhom et al (1987) is that H^+ ions bind within the conductance pore, altering its ionic environment. Although this might explain my data, the subconductance events that I observe are much longer (up to tens of ms at 0°C) than the very brief events described by Prodhom et al., and much more variable in amplitude than the longer subconductance events they produced by substitution of deuterium for hydrogen.

An alternative explanation is that subconductance levels in the Na^+ channel are due to small, transient conformational changes about the primary (i.e., most stable) open conformation. Such changes, by altering the internal structure of the pore, would alter its ability to conduct ions. Such conformational changes could be relatively long lived, especially at low temperatures. In addition, numerous sites might potentially be affected with different probabilities, giving rise to the diversity of states observed, as well as to the characteristic shape of the levels histogram. Tests of this and other hypotheses would require a more detailed understanding of factors that influence the amplitude and frequency of the sublevels. Nevertheless, one must conclude that the Na^+ channel, too, belongs in the category of channels that can conduct at many different levels.

REFERENCES

Auerbach, A., and F. Sachs. 1983. Flickering of a nicotinic ion channel to a subconductance state. *Biophysical Journal.* 42:1–10.

Bendat, J. S. and A. G. Piersol. 1986. Random Data: Analysis and Measurement Procedures. 2nd ed. Wiley-Interscience, New York. p. 83.

Cachelin, A. B., J. E. DePeyer, S. Kokubun, and H. Reuter. 1983. Sodium channels in cultured cardiac cells. *Journal of Physiology.* 340:389–401.

Chinn, K., and T. Narahashi. 1986. Stabilization of sodium channel states by deltamethrin in mouse neuroblastoma cells. *Journal of Physiology.* 380:191–207.

Colquhoun, D., and B. Sakmann. 1985. Fast events in single-channel currents activated by acetylcholine and its analogues at the frog muscle end-plate. *Journal of Physiology.* 369:501–557.

Colquhoun, D., and F. J. Sigworth. 1983. Fitting and statistical analysis of single-channel records. *In* Single Channel Recording. B. Sakmann, and E. Neher, editors. Plenum Publishing Corp., New York/London. 191–263.

Cull-Candy, S. G., and M. M. Usowicz. 1987. Multiple conductance channels activated by excitatory amino acids in cerebellar neurons. *Nature.* 325:525–528.

Garber, S. S., and C. Miller. 1987. Single Na^+ channels activated by veratradine and batrachotoxin. *Journal of General Physiology.* 89:459–480.

Gordon, L. G. M., and D. A. Haydon. 1972. The unit conductance channel of alamethicin. *Biochimica et Biophysica Acta.* 255:1014–1018.

Green, W. N., L. B. Weiss, and O. S. Andersen. 1987. Batrachotoxin-modified sodium channels in planar lipid bilayers: ion permeation and block. *Journal of General Physiology.* 89:841–872.

Hamill, O. P., J. Bormann, and B. Sakmann. 1983. Activation of multiple-conductance state chloride channels in spinal neurones by glycine and GABA. *Nature.* 305:805–808.

Hamill, O. P., and B. Sakmann. 1981. Multiple conductance states of single acetylcholine receptor channels in embryonic muscle cells. *Nature.* 294:462–464.

Hunter, M., and G. Giebisch. 1987. Multi-barrelled K$^+$ channels in renal tubules. *Nature.* 327:522–524.

Jahr, C. E., and C. F. Stevens. 1987. Glutamate activates multiple single channel conductances in hippocampal neurons. *Nature.* 325:522–525.

Kohlhardt, M., U. Frobe, and J. W. Herzig. 1986. Modifications of single cardiac Na$^+$ channels by DPI 201–106. *Journal of Membrane Biology.* 89:163–172.

Krouse, M. E., G. T. Schneider, and P. W. Gage. 1986. A large anion-selective channel has seven conductance levels. *Nature.* 319:58–60.

Labarca, P. P., and C. Miller. 1981. A K-selective, three-state channel from fragmented sarcoplasmic reticulum of frog leg muscle. *Journal of Membrane Biology.* 61:31–38.

Latorre, R., and O. Alvarez. 1981. Voltage dependent channels in lipid membranes. *Physiological Reviews.* 61:77–150.

Nagy, K. 1987. Subconductance states of single sodium channels modified by chloramine-T and sea anemone toxin in neuroblastoma cells. *European Biophysical Journal.* 15:129–132.

Nagy, K., and M. Bagany. 1986. Multiple discrete single sodium channel current levels in neuroblastoma cells. *Proceedings of the International Union of Physiological Sciences.* 16:441. (Abstr.)

Nagy, K., T. Kiss, and D. Hof. 1983. Single Na$^+$ channels in mouse neuroblastoma cell membrane. Indications for two open states. *Pflügers Archiv European Journal of Physiology.* 399:302–308.

Neher, E., and B. Sakmann. 1976. Single channel currents recorded from membrane of denervated frog muscle fibers. *Nature.* 260:799–802.

Noda, M., T. Ikeda, T. Kayano, H. Suzuki, H. Takeshima, M. Kurasaki, H. Takahashi, and S. Numa. 1986. Existence of distinct (sodium channel) messenger RNAs in rat brain. *Nature.* 320:188–192.

Patlak, J. B., and M. Ortiz. 1986. Two modes of gating during late Na$^+$ channel currents in frog sartorius muscle. *Journal of General Physiology.* 87:305–326.

Prodhom, B., D. Pietrobon, and P. Hess. 1987. Direct measurement of proton transfer rates to a group controlling the dihydropyridine-sensitive Ca^{++} channel. *Nature.* 329:243–246.

Romey, G., U. Quast, D. Pauron, C. Frelin, J. F. Renaud, and M. Lazdunski. 1987. Na$^+$ channels as sites of action of the cardioactive agent DPI 201-106 with agonist and antagonist enantiomers. *Proceedings of the National Academy of Science USA.* 84:896–900.

Scanley, B. E., and H. A. Fozzard. 1987. Low conductance sodium channels in canine cardiac Purkinje cells. *Biophysical Journal.* 52:489–495.

Scholtysik, G., R. Salzmann, R. Berthold, J. W. Herzig, U. Quast, and R. Markstein. 1985. DPI 201–106, a novel cardioactive agents: combination of cAMP-independent positive inotropic, negative chronotropic, action potential prolonging and coronary dilatory properties. *Naunyn-Schmiedeberg's Archiv für Pharmakologie.* 329:316–325.

Urban, B. W., E. Recio-Pinto, D. S. Duch, and M. Parnicas. 1987. Several conductance levels in steady state sodium channels. *Pflügers Archiv European Journal of Physiology.* 408:R311.

Vandenberg, C. A., and R. Horn. 1984. Inactivation viewed through single sodium channels. *Journal of General Physiology.* 84:535–564.

Weiss, R. E., and R. Horn. 1986. Single-channel studies of TTX-sensitive and TTX-resistant sodium channels in developing rat muscle reveal different open channel properties. *Annals of the New York Academy of Sciences.* 479:152–161.